Solving Discrete Dynamic Nonlinear Equation System Using New-Type DTG Model With Occasionally-Singular Jacobian Matrix

Binbin Qiu*‡, Jinjin Guo*‡, Xiaodong Li† and Yunong Zhang*‡
*School of Data and Computer Science, Sun Yat-sen University, Guangzhou 510006, China
†School of Intelligent Systems Engineering, Sun Yat-sen University, Guangzhou 510006, China
‡Research Institute of Sun Yat-sen University in Shenzhen, Shenzhen 518057, China
Email: zhynong@mail.sysu.edu.cn, ynzhang@ieee.org

***Abstract*—In this paper, a six-point discretization (6PD) formula is presented to discretize continuous-time models. Then, by using the 6PD formula and introducing the adaptivity/variability of parameter, a new-type discrete-time gradient (DTG) model is proposed to solve a discrete dynamic nonlinear equation system (DDNES) with occasionally-singular Jacobian matrix. For comparative purposes, based on the 6PD formula, a 6PD-type discrete-time zeroing (DTZ) model and an old-type (i.e., conventional) DTG model are also presented to handle the same problem. Finally, comparative numerical experiments, including an application to the discrete-time motion control of a robot manipulator, are conducted to substantiate the validity and superiority of the new-type DTG model for solving the DDNES with occasionally-singular Jacobian matrix. That is, when the Jacobian matrix of DDNES occasionally becomes singular as time evolves, the new-type DTG model can provide a feasible and effective solution to the singular Jacobian problem, whereas the other presented models fail to achieve such a solution.**

***Index Terms*—New-type discrete-time gradient model, discrete dynamic nonlinear equation system, adaptivity, robot manipulator, singular Jacobian problem**

I. Introduction

Over the past few decades, neural-dynamic approaches based on neural networks have become powerful alternatives to the online solution of mathematical and engineering problems [1]–[5]. Such approaches have some potential advantages, such as parallel processing [5], [6]. For example, a special class of recurrent neural dynamics, that is, zeroing neural dynamics (also called Zhang neural dynamics, ZND), has been proposed by Zhang *et al.* to solve various dynamic (or say, time-variant) problems [5]–[8]. Different from ZND, the typical gradient neural dynamics (GND), which has also been generalized to solve dynamic problems [1], [5], [7], [9], is designed intrinsically to solve time-invariant problems.

By utilizing the ZND and GND methods, previous studies [7], [10], [11] develop different continuous-time zeroing (CTZ) and continuous-time gradient (CTG) models to solve dynamic nonlinear equation systems. For the purposes of potential hardware realization and numerical algorithm development, the corresponding discrete-time models are also desirable to be developed and studied. For example, based on the classical Euler forward formula, discrete-time zeroing (DTZ) and discrete-time gradient (DTG) models are presented in [9] to solve dynamic nonlinear equations. Notably, previous studies associated with ZND or GND generally aim at solving dynamic nonlinear equation systems under the assumption that the corresponding Jacobian matrix is always nonsingular at any time instant regardless of continuous- or discrete-time models. Hence, many potential applications of these models (e.g., robot manipulators) may be considerably limited in some uncertain environments, wherein the Jacobian matrix may occasionally become singular as time evolves. Although some studies have reported on the means for solving the singular Jacobian problem of robot manipulators, such as the manipulability-maximizing schemes investigated in [12] and [13], these studies aim to avoid the singularity by maximizing the manipulability measure in a relatively complex and indirect manner. Thus, finding a simple and effective approach to conquer the singular Jacobian problem directly is an interesting research topic.

In this paper, a six-point discretization (6PD) formula is presented to discretize continuous-time models. Then, by using the 6PD formula and introducing the adaptivity/variability of parameter, a new-type DTG model is proposed to solve a discrete dynamic nonlinear equation system (DDNES) with occasionally-singular Jacobian matrix. For comparative purposes, on the basis of the 6PD formula, a 6PD-type DTZ model and an old-type DTG model are also presented to handle the same problem. Finally, comparative numerical experiments are conducted to substantiate the validity and superiority of the new-type DTG model for solving the DDNES with occasionally-singular Jacobian matrix.

Notably, although some achievements have been achieved for solving discrete dynamic problems, most studies are not up-to-date in academic research and practical applications. The main novelties and differences of this study from some relevant investigations are analyzed and summarized as follows to illustrate the highlights of the present work.

1) In [14], a class of prediction-correction models is proposed to solve dynamic convex optimization problem effectively. However, the corresponding Hessian matrix is required to be nonsingular at any time instant. In

978-1-7281-6926-2/20/$31.00 ©2020 IEEE

addition, given that the proposed prediction-correction models need to utilize future information in the correction step, it is thus difficult to apply them to strictly real-time applications in practice, where future information is generally unknown.

2) In [15], two DTZ models are proposed to solve future equation systems accurately in the presence of disturbance, whereas the investigation of a singular Jacobian problem as well as a practical application is still neglected. Moreover, the five-instant discretization formula adopted in [15] is quite different from the 6PD formula utilized in this study. Compared with the five-instant discretization formula, the 6PD formula is more stable for the discretization of continuous-time models.
3) In [16], based on the 6PD formula, a DTZ model is developed to solve future nonlinear minimization problem with high precision. Notably, this study is quite different from [16]. First, the investigated problems are different. Second, the singularity problem of the Hessian matrix in [16], which may be encountered during the problem-solving process, has not been explicitly considered and handled, not to mention a specific manipulator application verification.

The main contributions of this paper are refined and listed as follows.

1) Aiming to solve the DDNES with occasionally-singular Jacobian matrix, this work is remarkably different from previous studies on solving dynamic nonlinear equation systems generally with the stringent requirement of the Jacobian matrix being nonsingular at any time instant.
2) By introducing the adaptivity/variability of parameter, the new-type DTG model proposed for solving the DDNES can provide a feasible and effective solution to the singular Jacobian problem together with the corresponding manipulator application verification provided. Its design methodology can be used to elegantly cope with the system whose Jacobian matrix may occasionally become singular as time evolves.

II. Problem Description

The DDNES, which is to be solved at each computational time interval $[kp,(k+1)p) \subseteq [t_0,t_{\rm f}] \subseteq [0,+\infty)$, can be formulated as below [17]:

$$\mathbf{s}(\mathbf{r}_{k+1},t_{k+1})=\mathbf{0}\in\mathbb{R}^n, \tag{1}$$

where $t_{k+1}=(k+1)p$ with sampling period $p\in\mathbb{R}^+$ and updating index $k\in\mathbb{N}$; $\mathbf{s}(\cdot,\cdot):\mathbb{R}^n\times[0,+\infty)\to\mathbb{R}^n$ represents a differentiable dynamic nonlinear mapping function; t_0 and $t_{\rm f}$ denote the initial and final time instants, respectively. The future unknown solution $\mathbf{r}_{k+1}$ should be obtained during $[t_k$, $t_{k+1})$ based on the current- or prior-instant data to ensure that (1) holds true at the future/next time instant t_{k+1}.

To develop discrete-time models for solving DDNES (1), the following continuous dynamic nonlinear equation system is considered to be the continuation of (1):

$$\mathbf{s}\big(\mathbf{r}(t),t\big)=\mathbf{0}\in\mathbb{R}^n, \text{with } t\in[t_0,t_{\rm f}]\subseteq[0,+\infty). \tag{2}$$

III. 6PD-Type DTZ Model

According to the ZND design method [5], [6], we can obtain the following implicit CTZ model based on (2) [18]:

$$J(\mathbf{r}(t),t)\dot{\mathbf{r}}(t)=-\eta\mathbf{s}(\mathbf{r}(t),t)-\dot{\mathbf{s}}_t(\mathbf{r}(t),t), \tag{3}$$

where design parameter $\eta\in\mathbb{R}^+$. Besides, Jacobian matrix $J(\mathbf{r}(t),t)=\partial\mathbf{s}(\mathbf{r}(t),t)/\partial\mathbf{r}^{\rm T}(t)\in\mathbb{R}^{n\times n}$ and time-derivative vector $\dot{\mathbf{s}}_t(\mathbf{r}(t),t)=\partial\mathbf{s}(\mathbf{r}(t),t)/\partial t\in\mathbb{R}^n$. For further discretization, the implicit CTZ model (3) is transformed into the following explicit CTZ model:

$$\dot{\mathbf{r}}(t)=-H(\mathbf{r}(t),t)\big(\eta\mathbf{s}(\mathbf{r}(t),t)+\dot{\mathbf{s}}_t(\mathbf{r}(t),t)\big), \tag{4}$$

where $H(\mathbf{r}(t),t)$ refers to the inverse matrix of $J(\mathbf{r}(t),t)$ [17].

On the basis of Theorem 1 in [16], the 6PD formula is directly presented as below:

$$\begin{aligned}\dot{\mathbf{r}}_k\doteq&\frac{13}{24p}\mathbf{r}_{k+1}-\frac{1}{4p}\mathbf{r}_k-\frac{1}{12p}\mathbf{r}_{k-1}-\frac{1}{6p}\mathbf{r}_{k-2}\\&-\frac{1}{8p}\mathbf{r}_{k-3}+\frac{1}{12p}\mathbf{r}_{k-4},\end{aligned} \tag{5}$$

which has a truncating error of $\mathbf{O}(p^3)$ with every element being $\mathcal{O}(p^3)$, and "$\doteq$" denotes the computational assignment operation [17].

By applying the 6PD formula (5) to discretize the CTZ model (4), and using a four-point backward difference rule to approximate the time-derivative term, the 6PD-type DTZ model is finally obtained as follows [17]:

$$\begin{aligned}\mathbf{r}_{k+1}\doteq&\frac{6}{13}\mathbf{r}_k+\frac{2}{13}\mathbf{r}_{k-1}+\frac{4}{13}\mathbf{r}_{k-2}+\frac{3}{13}\mathbf{r}_{k-3}\\&-\frac{2}{13}\mathbf{r}_{k-4}-\frac{24}{13}H(\mathbf{r}_k,t_k)\big(h\mathbf{s}(\mathbf{r}_k,t_k)+\Delta\mathbf{s}(\mathbf{r}_k,t_k)\big),\end{aligned} \tag{6}$$

where stepsize $h=p\eta\in\mathbb{R}^+$, and

$$\begin{aligned}\Delta\mathbf{s}(\mathbf{r}_k,t_k)=&\frac{11}{6}\mathbf{s}(\mathbf{r}_k,t_k)-3\mathbf{s}(\mathbf{r}_k,t_{k-1})\\&+\frac{3}{2}\mathbf{s}(\mathbf{r}_k,t_{k-2})-\frac{1}{3}\mathbf{s}(\mathbf{r}_k,t_{k-3}).\end{aligned}$$

IV. New-Type DTG Model

It is worth particularly pointing out that the 6PD-type DTZ model (6) may no longer be valid if the corresponding Jacobian matrix occasionally becomes singular as time evolves. Accordingly, the new-type DTG model, which is an effective solution approach to the singular Jacobian problem, is proposed in this section. In addition, the old-type (i.e., conventional) DTG model is also presented for further comparison.

Based on the GND design method [1], the following old-type CTG model is revisited and presented [9], [10]:

$$\dot{\mathbf{r}}(t)=-\gamma J^{\rm T}(\mathbf{r}(t),t)\mathbf{s}(\mathbf{r}(t),t), \tag{7}$$

where superscript $^{\rm T}$ denotes the transpose operator and design parameter $\gamma\in\mathbb{R}^+$. However, as stated in [10], the old-type CTG model cannot provide an accurate solution to the dynamic nonlinear equation with a relatively large residual error. Therefore, the adaptivity/variability of parameter is introduced

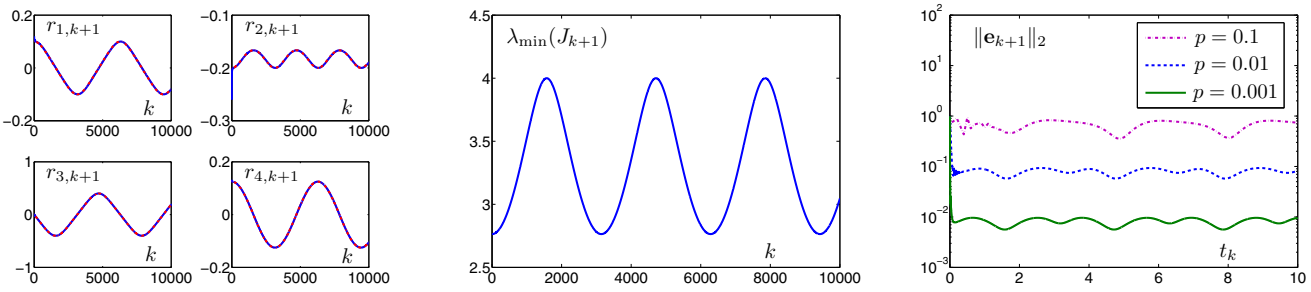

(a) (b) (c)

Fig. 1. Convergence performance of new-type DTG model (9) for solving DDNES (11)-(12) in Situation I. (a) Element trajectories of state vector $\mathbf{r}_{k+1}$ (denoted by blue solid curves) with $p = 0.001$ s. (b) Minimal eigenvalue of Jacobian matrix $J(\mathbf{r}_{k+1}, t_{k+1})$ with $p = 0.001$ s. (c) Residual errors $\|\mathbf{e}_{k+1}\|_2$ with different p values.

to address the weakness of the old-type CTG model (7), and then the new-type CTG model with an adaptive parameter is designed as below:

$$\dot{\mathbf{r}}(t) = -\alpha(t)J^{\mathrm{T}}(\mathbf{r}(t), t)\mathbf{s}(\mathbf{r}(t), t), \tag{8}$$

where the adaptive parameter $\alpha(t) \in \mathbb{R}^+$. By applying the 6PD formula (5) to discretize the new-type CTG model (8), the new-type DTG model is then obtained as below:

$$\begin{aligned}\mathbf{r}_{k+1} \doteq & \frac{6}{13}\mathbf{r}_k + \frac{2}{13}\mathbf{r}_{k-1} + \frac{4}{13}\mathbf{r}_{k-2} + \frac{3}{13}\mathbf{r}_{k-3} \\ & - \frac{2}{13}\mathbf{r}_{k-4} - \frac{24}{13}h_k J^{\mathrm{T}}(\mathbf{r}_k, t_k)\mathbf{s}(\mathbf{r}_k, t_k),\end{aligned} \tag{9}$$

where stepsize $h_k = p\alpha_k \in \mathbb{R}^+$. Notably, h should satisfy $0 < h < 2/\mathrm{trace}(J^{\mathrm{T}}J)$ to facilitate the calculation for time-invariant problem solving; or more rigorously, $0 < h < 2/\lambda_{\max}(J^{\mathrm{T}}J)$, where $\lambda_{\max}(J^{\mathrm{T}}J)$ denotes the largest eigenvalue of matrix $J^{\mathrm{T}}J$ [2]. For simplicity, $h_k = 1/\mathrm{trace}(J^{\mathrm{T}}(\mathbf{r}_k, t_k)J(\mathbf{r}_k, t_k))$ is utilized in (9) [2], where $\alpha_k = 1/(p\mathrm{trace}(J^{\mathrm{T}}(\mathbf{r}_k, t_k)J(\mathbf{r}_k, t_k)))$.

Moreover, as indicated in [19], when exploited for solving a discrete dynamic system of linear equations, the MSRE of any method designed intrinsically for solving the time-invariant one is of order $\mathcal{O}(p)$. Generalized from the above, the following theoretical result can be obtained.

Proposition 1: If the new-type DTG model (9) is used to solve DDNES (1) with Jacobian matrix $J(\mathbf{r}_k, t_k)$ being nonsingular and uniformly bounded during $[t_0, t_{\mathrm{f}}]$ and with sampling period $p \in (0, 1)$, then its MSRE $\lim_{k\to\infty} \sup \|\mathbf{s}(\mathbf{r}_{k+1}, t_{k+1})\|_2$ is of order $\mathcal{O}(p)$.

As shown in the subsequent section, the new-type DTG model (9) can provide a feasible and effective solution to the singular Jacobian problem. Hence, the following theoretical results are provided accordingly.

Proposition 2: If the new-type DTG model (9) is used to solve DDNES (1) with Jacobian matrix $J(\mathbf{r}_k, t_k)$ occasionally becoming singular during $[t_0, t_{\mathrm{f}}]$ and with sampling period $p \in (0, 1)$, then the following two results could be obtained.

1) When k lies in nonsingular time index intervals, the new-type DTG model (9) is stable and convergent, and its MSRE $\lim_{k\to\infty} \sup \|\mathbf{s}(\mathbf{r}_{k+1}, t_{k+1})\|_2$ is of order $\mathcal{O}(p)$.
2) When k lies in singular time index intervals, the new-type DTG model (9) is still stable, and its MSRE $\lim_{k\to\infty} \sup \|\mathbf{s}(\mathbf{r}_{k+1}, t_{k+1})\|_2$ is bounded.

For further illustration, by discretizing the old-type CTG model (8) with the 6PD formula (5), the following old-type DTG model is obtained:

$$\begin{aligned}\mathbf{r}_{k+1} \doteq & \frac{6}{13}\mathbf{r}_k + \frac{2}{13}\mathbf{r}_{k-1} + \frac{4}{13}\mathbf{r}_{k-2} + \frac{3}{13}\mathbf{r}_{k-3} \\ & - \frac{2}{13}\mathbf{r}_{k-4} - \frac{24}{13}hJ^{\mathrm{T}}(\mathbf{r}_k, t_k)\mathbf{s}(\mathbf{r}_k, t_k),\end{aligned} \tag{10}$$

where stepsize $h = p\gamma \in \mathbb{R}^+$. Numerical comparison with the old-type DTG model (10) is further conducted in the later section to substantiate the peculiarity of the new-type DTG model (9).

V. Numerical Experiments and Comparisons

In this section, illustrative examples are provided to substantiate the validity and superiority of the new-type DTG model (9) for solving the DDNES with occasionally-singular Jacobian matrix.

Example 1: Consider the following DDNES with the future unknown solution $\mathbf{r}_{k+1}$ to be obtained at each computational time interval $[kp, (k+1)p) \subseteq [0, 10]$:

$$\mathbf{s}(\mathbf{r}_{k+1}, t_{k+1}) = \mathbf{0} \in \mathbb{R}^4 \tag{11}$$

with

$$\mathbf{s}(\mathbf{r}_k, t_k) = \begin{bmatrix} 4r_{1,k} + 2\cos(t_k)r_{2,k} \\ 6r_{2,k} + 2\cos(t_k)r_{1,k} + 1 \\ 2w(t_k)r_{3,k} + 4\sin(t_k) \\ 8r_{4,k} - \cos(t_k) \end{bmatrix}, \tag{12}$$

where $\mathbf{r}_k = [r_{1,k}, r_{2,k}, r_{3,k}, r_{4,k}]^{\mathrm{T}}$ with $r_{i,k}$ denoting its ith element, and $w(t_k)$ contains two situations to be discussed as follows. For solving DDNES (11)-(12), we set the sampling period $p = 0.1$, 0.01 or 0.001 s, and stepsize $h = 0.3$ for the 6PD-type DTZ model (6) as well as $h_k = 1/\mathrm{trace}\big(J^{\mathrm{T}}(\mathbf{r}_k, t_k)J(\mathbf{r}_k, t_k)\big)$ for the new-type DTG model (9) in default.

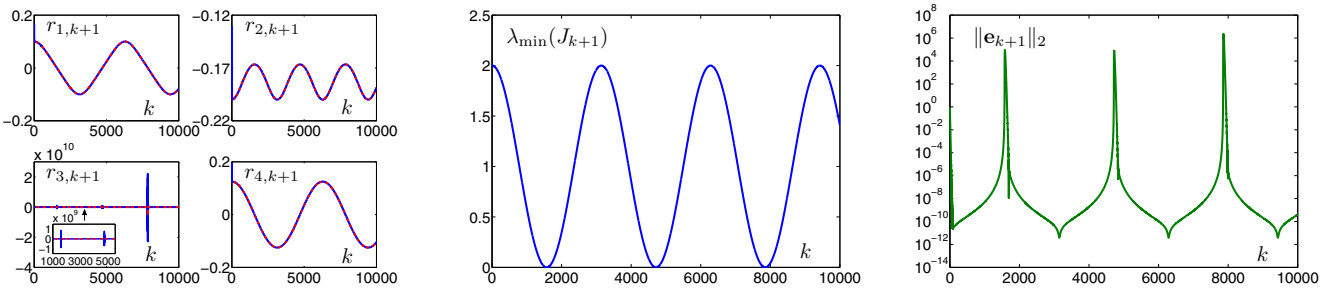

(a) (b) (c)

Fig. 2. Convergence performance of 6PD-type DTZ model (6) with $p = 0.001$ s for solving DDNES (11)-(12) in Situation II. (a) Element trajectories of state vector $\mathbf{r}_{k+1}$ (denoted by blue solid curves). (b) Minimal eigenvalue of Jacobian matrix $J(\mathbf{r}_{k+1}, t_{k+1})$. (c) Residual error $\|\mathbf{e}_{k+1}\|_2$.

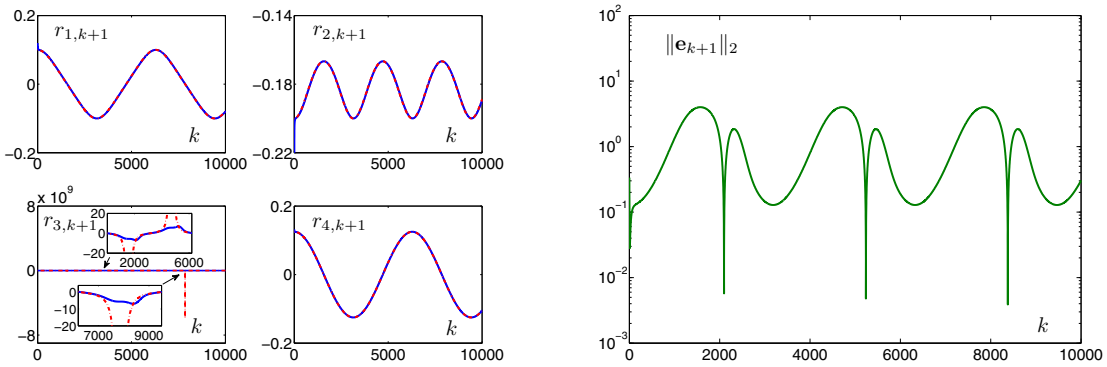

(a) (b)

Fig. 3. Convergence performance of new-type DTG model (9) with $p = 0.001$ s for solving DDNES (11)-(12) in Situation II. (a) Element trajectories of state vector $\mathbf{r}_{k+1}$ (denoted by blue solid curves). (b) Residual error $\|\mathbf{e}_{k+1}\|_2$.

Situation I: With $w(t_k) = 6 - \sin^2(t_k)$ in DDNES (11)-(12). The corresponding numerical results are shown in Fig. 1. As illustrated in Fig. 1(a), synthesized by the new-type DTG model (9), the element trajectories of state vector $\mathbf{r}_{k+1}$ (denoted by blue solid curves) rapidly converge to the theoretical solution $\mathbf{r}^*_{k+1}$ (denoted by red dash-dotted curves). As shown in Fig. 1(b), the minimal eigenvalue of $J(\mathbf{r}_{k+1}, t_{k+1})$ for DDNES (11)-(12) in Situation I is always larger than zero, thereby implying that the Jacobian matrix is nonsingular for all $t_k \in [0, 10]$. In addition, the residual errors $\|\mathbf{e}_{k+1}\|_2 = \|\mathbf{s}(\mathbf{r}_{k+1}, t_{k+1})\|_2$ of the new-type DTG model (9) with different p values are displayed in Fig. 1(c). As depicted in Fig. 1(c), the MSRE of (9) reduces by 10 times as the value of p decreases by 10 times. That is, the MSRE of (9) changes in the manner of $\mathcal{O}(p)$, which is consistent with the theoretical result presented in Proposition 1.

Situation II: With $w(t_k) = \cos^2(t_k)$ in DDNES (11)-(12). In this situation, the Jacobian matrix is formulated as

$$J(\mathbf{r}_k, t_k) = \begin{bmatrix} 4 & 2\cos(t_k) & 0 & 0 \\ 2\cos(t_k) & 6 & 0 & 0 \\ 0 & 0 & 2\cos^2(t_k) & 0 \\ 0 & 0 & 0 & 8 \end{bmatrix}, \quad (13)$$

which becomes singular at time instants $t_s = (2\kappa + 1)\pi/2$ s with $\kappa = 0, 1, 2, \ldots$. That is, Jacobian matrix (13) is sometimes nonsingular but sometimes singular. As the solution duration $T = 10$ s, there thus exist three singular time instants in the entire computational process, that is, $t_{s1} = \pi/2 \approx 1.571$ s, $t_{s2} = 3\pi/2 \approx 4.712$ s, and $t_{s3} = 5\pi/2 \approx 7.854$ s. The corresponding numerical results are shown in Figs. 2 and 3.

Specifically, Fig. 2 displays the convergence performance of 6PD-type DTZ model (6) for solving DDNES (11)-(12) in Situation II. As illustrated in Fig. 2(a), the trajectories of three elements of state vector $\mathbf{r}_{k+1}$ (i.e., $r_{1,k+1}$, $r_{2,k+1}$, and $r_{4,k+1}$) rapidly converge to the corresponding three elements of theoretical solution $\mathbf{r}^*_{k+1}$. However, the magnitude of the third element of state vector $\mathbf{r}_{k+1}$ abruptly becomes extremely large (i.e., of order 10^9 or 10^{10}) at the three singular time instants t_{s1}, t_{s2}, and t_{s3}. It can also be verified from Fig. 2(b) that the minimal eigenvalue of $J(\mathbf{r}_{k+1}, t_{k+1})$ for DDNES (11)-(12) in Situation II becomes zero at such three time instants; that is, the corresponding Jacobian matrix becomes singular at the three time instants. Moreover, Fig. 2(c) demonstrates that the residual error $\|\mathbf{e}_{k+1}\|_2$ synthesized by the 6PD-type DTZ model (6) becomes extremely large at the three singular time index intervals, which is order 10^4 or 10^6. The above

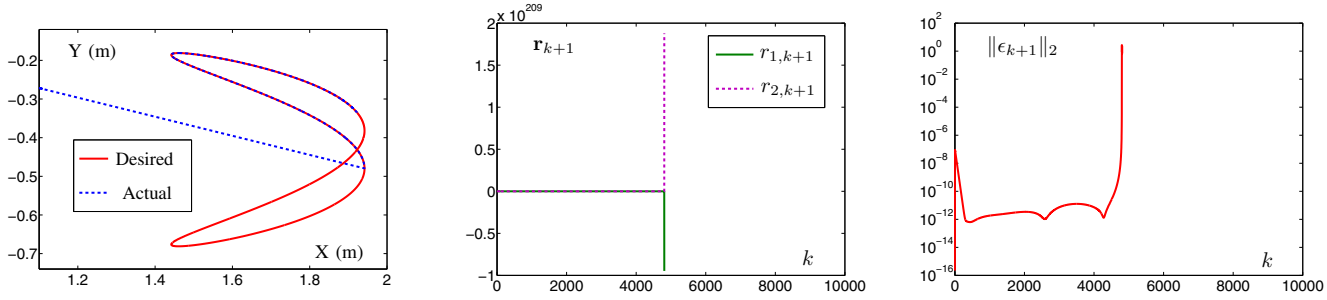

(a) (b) (c)

Fig. 4. DDNES (14)-(15) in Situation I equipped with 6PD-type DTZ model (6) for two-link robot manipulator with its end-effector tracking Lissajous-figure path. (a) Desired path and actual trajectory. (b) Joint-velocity vector $\mathbf{r}_{k+1}$. (c) Tracking error $\|\epsilon_{k+1}\|_2$.

numerical results reveal that the 6PD-type DTZ model (6) is less feasible or less effective for solving DDNES (11)-(12) in Situation II, where the corresponding Jacobian matrix occasionally becomes singular as time evolves.

In contrast, the convergence performance of the new-type DTG model (9) for solving DDNES (11)-(12) in Situation II is shown in Fig. 3. As seen from Fig. 3(a), the trajectories of three elements of state vector $\mathbf{r}_{k+1}$ (i.e., $r_{1,k+1}$, $r_{2,k+1}$, and $r_{4,k+1}$) all converge rapidly to the corresponding three elements of theoretical solution $\mathbf{r}^*_{k+1}$. Notably, unlike the 6PD-type DTZ model (6), the trajectory of the third element of state vector $\mathbf{r}_{k+1}$ synthesized by the new-type DTG model (9) is smooth and does not suffer from abrupt changes to extremely large values at the three singular time instants t_{s1}, t_{s2}, and t_{s3}. Furthermore, Fig. 3(b) illustrates that the residual error $\|\mathbf{e}_{k+1}\|_2$ synthesized by the new-type DTG model (9) is still sufficiently small (i.e., of order 10^0). This error is considerably smaller than that synthesized by the 6PD-type DTZ model (6) shown in Fig. 2(c), even at the three singular time index intervals. In view of the above numerical results for solving DDNES (11)-(12) in Situation II, it can be found that the new-type DTG model (9) provides a feasible and effective solution to the singular Jacobian problem. Hence, an important advantage of the new-type DTG model over the 6PD-type DTZ model is that the former is capable of conquering the singular Jacobian problem effectively and elegantly when solving DDNES (11)-(12) in Situation II.

Example 2: For a two-link robot manipulator, at time instant $t_k \in [0, t_f]$, the position-level kinematic equation is $\phi(\theta_k) = \mathbf{c}_k$, where $\theta_k \in \mathbb{R}^2$ and $\mathbf{c}_k \in \mathbb{R}^2$ denote the joint-angle vector and the end-effector position vector, respectively. Besides, $\phi(\cdot)$ denotes the forward-kinematic nonlinear mapping function [13], [20]. Then, the velocity-level kinematic equation is $J_k\mathbf{r}_k = \dot{\mathbf{c}}_k \to \dot{\mathbf{c}}^{\mathrm{d}}_k$, where $\mathbf{r}_k = \dot{\theta}_k$, $\dot{\mathbf{c}}_k$, J_k, and $\dot{\mathbf{c}}^{\mathrm{d}}_k$ denote the joint-velocity vector, the end-effector velocity vector, the robot Jacobian matrix, and the time derivative of the end-effector desired path, respectively [17], [21]. The discrete-time motion control problem of robot manipulators [13] can be expressed as the following DDNES with $\mathbf{r}_{k+1}$ to be obtained at each computational time interval $[kp, (k+1)p) \subseteq [0, t_f]$:

$$\mathbf{s}(\mathbf{r}_{k+1}, t_{k+1}) = \mathbf{0} \in \mathbb{R}^2 \tag{14}$$

with

$$\mathbf{s}(\mathbf{r}_k, t_k) = J_k\mathbf{r}_k - \dot{\mathbf{c}}^{\mathrm{d}}_k - \sigma(\mathbf{c}^{\mathrm{d}}_k - \mathbf{c}_k), \tag{15}$$

where σ is a positive feedback-gain coefficient. For solving DDNES (14)-(15), one can set $t_f = 10$ s, $p = 0.001$ s, and $h = 0.3$ for the 6PD-type DTZ model (6) as well as $h_k = 3/(5\mathrm{trace}(J_k^{\mathrm{T}}J_k))$ for the new-type DTG model (9). Then, different initial joint-angle vectors θ_0 are chosen to solve DDNES (14)-(15) with occasionally-singular Jacobian matrix.

Situation I: With $\theta_0 = [-\pi/8, 11/25]^{\mathrm{T}}$ rad for DDNES (14)-(15). The corresponding numerical results are shown in Figs. 4 and 5. As seen from Fig. 4, the Lissajous-figure-path tracking task equipped with the 6PD-type DTZ model (6) fails as time evolves. Specifically, this task collapses at time instant $t_s \approx 4.848$ s when the robot Jacobian matrix becomes singular, which can be verified from Fig. 5(b). Notably, the actual trajectory is consistent with the desired Lissajous-figure path before the singular time instant t_s, as shown in Fig. 4(a). These numerical results indicate that the 6PD-type DTZ model (6) is less applicable for solving DDNES (14)-(15) in Situation I whose robot Jacobian matrix occasionally becomes singular as time evolves. In contrast, Fig. 5(a) demonstrates that the Lissajous-figure-path tracking task equipped with the new-type DTG model (9) runs uninterruptedly as time evolves. Moreover, although a slight offset exists around the singular time instant t_s, the actual trajectory tracks the desired Lissajous-figure path well. Hence, the new-type DTG model (9) can also achieve convergence even in the presence of a singular Jacobian matrix. Furthermore, as illustrated in Fig. 5(c), the joint-velocity profiles are smooth and become zero at the end of the motion. From Fig. 5(d), one can observe that the maximal tracking error $\|\epsilon_{k+1}\|_2$ is sufficiently small (i.e., of order 10^{-3} m) for engineering applications. This finding implies that the Lissajous-figure-path tracking task equipped with the new-type DTG model (9) for solving DDNES (14)-(15) in Situation I is successfully fulfilled. Thus, the capability of new-type DTG model (9) for conquering the singular Jacobian problem is substantiated primarily.

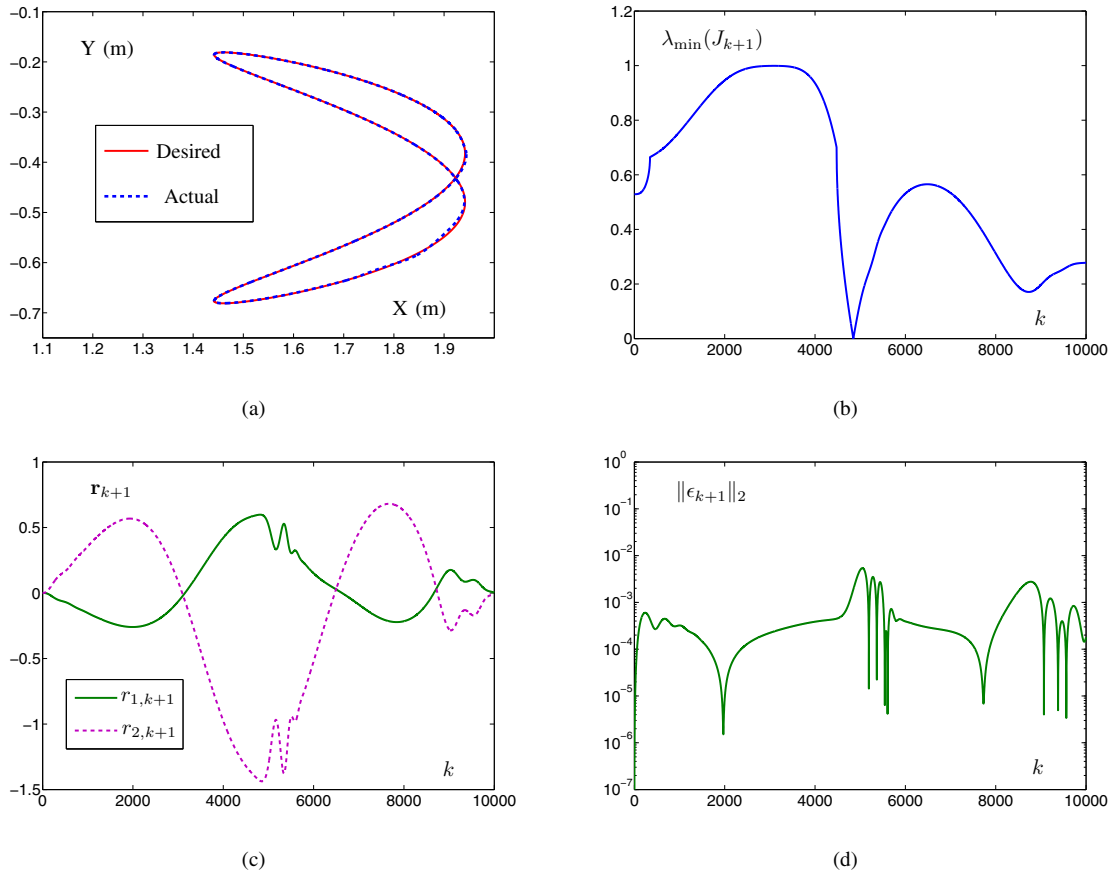

Fig. 5. DDNES (14)-(15) in Situation I equipped with new-type DTG model (9) for two-link robot manipulator with its end-effector tracking Lissajous-figure path. (a) Desired path and actual trajectory. (b) Minimal absolute eigenvalue of robot Jacobian matrix J_{k+1}. (c) Joint-velocity vector $\mathbf{r}_{k+1}$. (d) Tracking error $\|\epsilon_{k+1}\|_2$.

Situation II: With $\theta_0 = [-\pi/8, \pi/8]^{\mathrm{T}}$ rad for DDNES (14)-(15). In this situation, the capability of new-type DTG model (9) for conquering the singular Jacobian problem with more than one singular direction is illustrated. The corresponding numerical results are shown in Fig. 6. Specifically, As presented in Fig. 6(a), the Lissajous-figure-path tracking task equipped with the new-type DTG model (9) runs uninterruptedly as time evolves. Moreover, although small offsets exist when the robot Jacobian matrix becomes singular at the three time instants of $t_{s1} \approx 4.706$ s, $t_{s2} \approx 5.020$ s, and $t_{s3} \approx 8.636$ s (as verified from Fig. 6(b)), the actual trajectory tracks the desired Lissajous-figure path well. Besides, as shown in Fig. 6(c), even at the three singular time index intervals, the maximal tracking error $\|\epsilon_{k+1}\|_2$ synthesized by the new-type DTG model (9) is also small (i.e., of order 10^{-2} or 10^{-3} m), which is acceptable in engineering applications. However, similar to the above Situation II of DDNES (14)-(15), the corresponding numerical results indicate that the 6PD-type DTZ model (6) is also less applicable for solving DDNES (14)-(15) in Situation II. These results are omitted here due to similarity. Therefore, the capability of new-type DTG model (9) for conquering the singular Jacobian problem is substantiated once more.

Remark 1: The comparisons on different schemes designed to overcome the singular Jacobian problem of robot manipulators are summarized in Table I to further illustrate the advantages of new-type DTG model (9). In [13], a manipulability optimization scheme and its dynamical neural network (DNN) solver are proposed. The comparisons in Table I show that the scheme proposed in [13] aims to cope with the singular Jacobian problem indirectly by maximizing the manipulability measure. By contrast, although multiple singularities exist, the new-type DTG model (9) proposed in this paper can directly and effectively conquer the singular Jacobian problem encountered in the path-tracking process. Furthermore, the design procedure and formulation of the scheme proposed in [13] are substantially more complicated than those of new-type DTG model (9); thus, the former may suffer from a heavy computing burden and require considerably long computational time to fulfill the motion control task of robot manipulators. Moreover, in [13], the continuous-time scheme and its solver are developed to deal with the manipulability optimization problem of robot manipulators. However, their industrial implementation in digital hardware may be more difficult than the discrete-time counterparts. By contrast, the new-type DTG model proposed in this paper can successfully

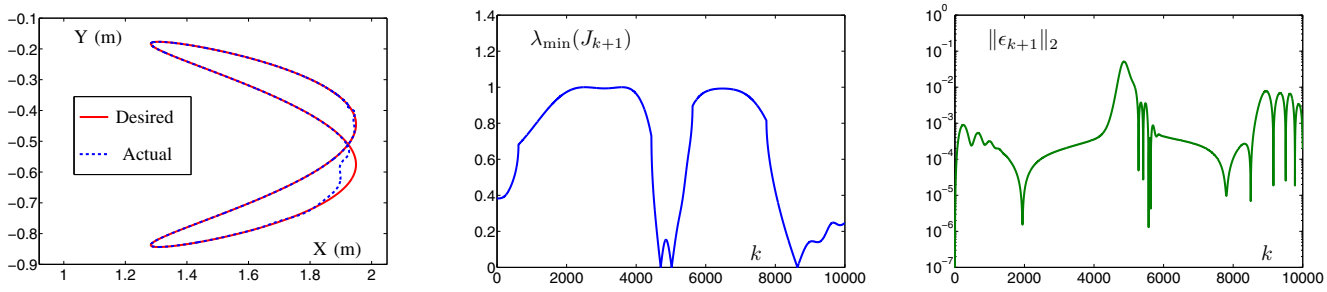

(a) (b) (c)

Fig. 6. DDNES (14)-(15) in Situation II equipped with new-type DTG model (9) for two-link robot manipulator with its end-effector tracking Lissajous-figure path. (a) Desired path and actual trajectory. (b) Minimal absolute eigenvalue of robot Jacobian matrix J_{k+1}. (c) Tracking error $\|\epsilon_{k+1}\|_2$.

TABLE I
COMPARISONS ON DIFFERENT SCHEMES DESIGNED FOR COPING WITH SINGULAR JACOBIAN PROBLEM OF ROBOT MANIPULATORS

	Solver	Discrete vs. continuous	Design procedure	Computing burden	Tracking error	Singularity handling
This paper	new-type DTG model (9)	Discrete	Simple	Little	Small	Yes (indirectly)
[13]	DNN (39) in [13]	Continuous	Complex	Heavy	Small	Yes (directly)

fulfill the discrete-time motion control task of robot manipulators formulated as a DDNES, together with the singular Jacobian problem conquered elegantly and directly.

Remark 2: As previously presented, by introducing the adaptivity/variability of parameter and applying the 6PD formula (5) to discretize the new-type CTG model (8), the new-type DTG model (9) is proposed to solve the DDNES, and two illustrative examples have shown that it provides a feasible and effective solution to the singular Jacobian problem. For further illustration, we also verify such a peculiarity of new-type DTG model (9) by making a comparison with the old-type DTG model (10). In the following, Example 1 in Situation II and Example 2 in Situation I are further investigated by exploiting the old-type DTG model (10) under the same conditions, with the corresponding numerical results shown in Fig. 7. As seen from the figure, when the old-type DTG model (10) is used to solve the corresponding DDNES of Example 1 in Situation II and Example 2 in Situation I, the undesired divergence phenomena occur from the beginning of the solution process. This occurrence means that the old-type DTG model (10) cannot achieve convergence to the theoretical solution even before the singular time instant, not to mention increasingly challenging situation of conquering the singular Jacobian problem. All the above comparative numerical results indicate that the new-type DTG model (9) is capable of conquering the singular Jacobian problem and can also achieve convergence even in the presence of a singular Jacobian matrix.

VI. CONCLUSION

In this paper, by using the 6PD formula (5) and introducing the adaptivity/variability of parameter, the new-type DTG model (9) has been proposed to solve the DDNES with occasionally-singular Jacobian matrix. For comparative purposes, based on the 6PD formula (5), the 6PD-type DTZ model (6) and the old-type DTG model (10) have also been presented to handle the same problem. Finally, comparative numerical results have substantiated the validity and superiority of the new-type DTG model for solving the DDNES with occasionally-singular Jacobian matrix. Applying the proposed design methodology to the more complex dynamic behavior of discrete nonlinear systems could be an interesting research direction in the future.

ACKNOWLEDGMENT

This work was supported in part by the National Natural Science Foundation of China under Grant 61976230, in part by the China Postdoctoral Science Foundation under Grant 2018M643306, in part by the Guangdong Basic and Applied Basic Research Foundation under Grant 2019A1515012128, in part by the Fundamental Research Funds for the Central Universities under Grant 19lgpy227, and in part by the Shenzhen Science and Technology Plan Project under Grant JCYJ20170818154936083.

REFERENCES

[1] Y. Zhang, K. Chen, and H. Tan, "Performance analysis of gradient neural network exploited for online time-varying matrix inversion," *IEEE Trans. Autom. Control*, vol. 54, no. 8, pp. 1940–1945, Aug. 2009.

[2] Y. Zhang, B. Mu, and H. Zheng, "Link between and comparison and combination of Zhang neural network and quasi-Newton BFGS method for time-varying quadratic minimization," *IEEE Trans. Cybern.*, vol. 43, no. 2, pp. 490–503, Apr. 2013.

[3] S. Qin, J. Feng, J. Song, X.Wen, and C. Xu, "A one-layer recurrent neural network for constrained complex-variable convex optimization," *IEEE Trans. Neural Netw. Learn. Syst.*, vol. 29, no. 3, pp. 534–544, Mar. 2018.

[4] L. Jin, S. Li, B. Hu, M. Liu, and J. Yu, "A noise-suppressing neural algorithm for solving the time-varying system of linear equations: A control-based approach," *IEEE Trans. Ind. Inform.*, vol. 15, no. 1, pp. 236–246, Jan. 2019.

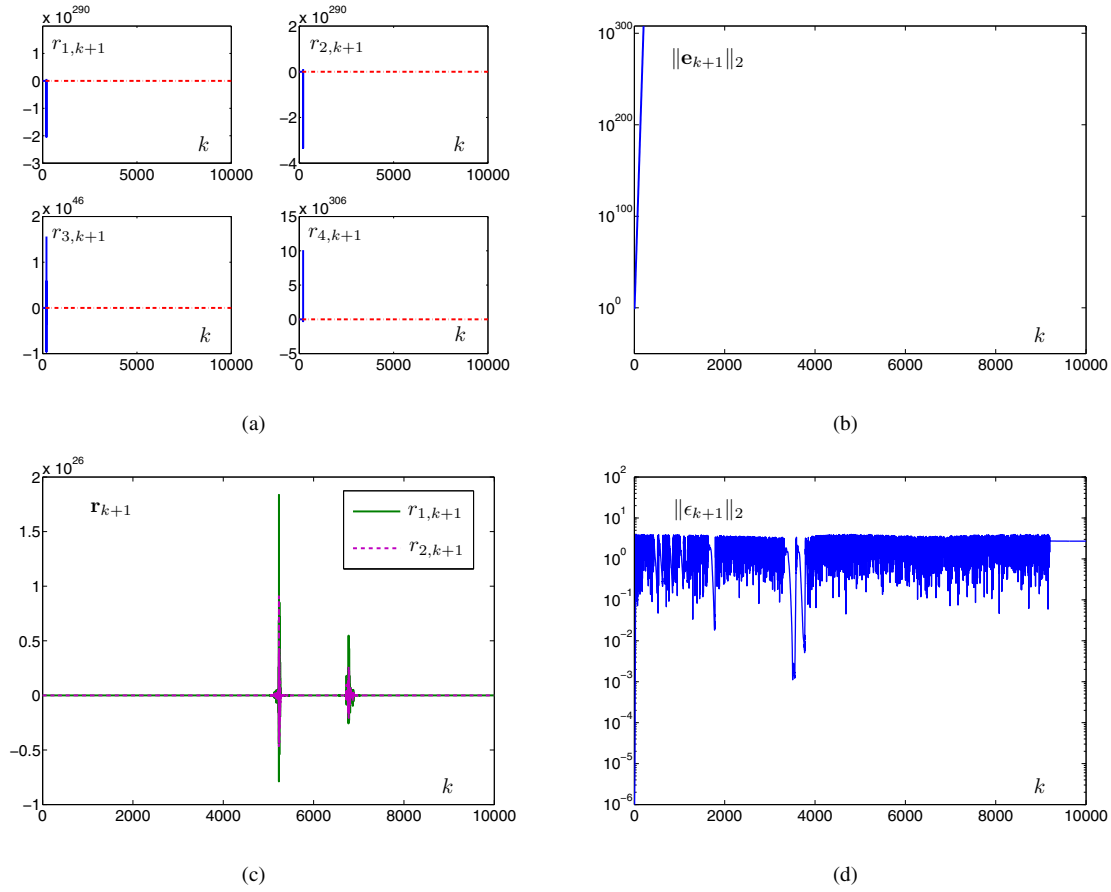

Fig. 7. Divergence phenomena occurring during solution process with old-type DTG model (10) used for DDNES solving. (a) Element trajectories of state vector $\mathbf{r}_{k+1}$ (denoted by blue solid curves) for Example 1 in Situation II. (b) Residual error $\|\mathbf{e}_{k+1}\|_2$ for Example 1 in Situation II. (c) Joint-velocity vector $\mathbf{r}_{k+1}$ for Example 2 in Situation I. (d) Tracking error $\|\epsilon_{k+1}\|_2$ for Example 2 in Situation I.

[5] Y. Zhang, L. Xiao, Z. Xiao, and M. Mao, *Zeroing Dynamics, Gradient Dynamics, and Newton Iterations*. Boca Raton, FL, USA: CRC Press, 2015.

[6] Y. Zhang and C. Yi, *Zhang Neural Networks and Neural-Dynamic Method*. New York, NY, USA: Nova Science Publishers, 2011.

[7] L. Xiao, "A nonlinearly activated neural dynamics and its finite-time solution to time-varying nonlinear equation," *Neurocomputing*, vol. 173, pp. 1983–1988, Jan. 2016.

[8] D. Guo, Z. Nie, and L. Yan, "Theoretical analysis, numerical verification and geometrical representation of new three-step DTZD algorithm for time-varying nonlinear equations solving," *Neurocomputing*, vol. 214, pp. 516–526, Nov. 2016.

[9] Y. Zhang, Z. Li, D. Guo, Z. Ke, and P. Chen, "Discrete-time ZD, GD and NI for solving nonlinear time-varying equations," *Numer. Algorithms*, vol. 64, no. 4, pp. 721–740, Dec. 2013.

[10] Y. Zhang, C. Yi, D. Guo, and J. Zheng, "Comparison on Zhang neural dynamics and gradient-based neural dynamics for online solution of nonlinear time-varying equation," *Neural Comput. Appl.*, vol. 20, no. 1, pp. 1–7, Feb. 2011.

[11] Y. Zhang, Y. Shi, L. Xiao, and B. Mu, "Convergence and stability results of Zhang neural network solving systems of time-varying nonlinear equations," in *Proc. Int. Conf. Nat. Comput.*, Chongqing, China, 2012, pp. 143–147.

[12] B. Bayle, J.-Y. Fourquet, and M. Renaud, "Manipulability of wheeled mobile manipulators: Application to motion generation," *Int. J. Robot. Res.*, vol. 22, no. 7–8, pp. 565–581, Jul.–Aug. 2003.

[13] L. Jin, S. Li, H. M. La, and X. Luo, "Manipulability optimization of redundant manipulators using dynamic neural networks," *IEEE Trans. Ind. Electron.*, vol. 64, no. 6, pp. 4710–4720, Jun. 2017.

[14] A. Simonetto, A. Mokhtari, A. Koppel, G. Leus, and A. Ribeiro, "A class of prediction-correction methods for time-varying convex optimization," *IEEE Trans. Signal Process.*, vol. 64, no. 17, pp. 4576–4591, Sep. 2016.

[15] Y. Shi and Y. Zhang, "Solving future equation systems using integral-type error function and using twice ZNN formula with disturbances suppressed," *J. Franklin Inst.*, vol. 356, no. 4, pp. 2130–2152, Mar. 2019.

[16] B. Qiu, Y. Zhang, J. Guo, Z. Yang, and X. Li, "New five-step DTZD algorithm for future nonlinear minimization with quartic steady-state error pattern," *Numer. Algorithms*, vol. 81, no. 3, pp. 1043–1065, Jul. 2019.

[17] J. Guo, B. Qiu, and Y. Zhang, "New-type DTZ model for solving discrete time-dependent nonlinear equation system with robotic-arm application," in *Proc. Int. Conf. Inf. Sci. Technol.*, 2020, accepted.

[18] Y. Zhang, C. Peng, W. Li, Y. Shi, and Y. Ling, "Broyden-method aided discrete ZNN solving the systems of time-varying nonlinear equations," in *Proc. Int. Conf. Control Eng. Commun. Technol.*, Shenyang, China, 2012, pp. 492–495.

[19] L. Jin, Y. Zhang, and B. Qiu, "Neural network-based discrete-time Z-type model of high accuracy in noisy environments for solving dynamic system of linear equations," *Neural Comput. Appl.*, vol. 29, no. 11, pp. 1217–1232, Jun. 2018.

[20] B. Qiu, Y. Zhang, and Z. Yang, "Analysis, verification and comparison on feedback-aided Ma equivalence and Zhang equivalency of minimum-kinetic-energy type for kinematic control of redundant robot manipulators," *Asian J. Control*, vol. 20, no. 6, pp. 2154–2170, Nov. 2018.

[21] B. Qiu, Y. Zhang, and Z. Yang, "Revisit and compare Ma equivalence and Zhang equivalence of minimum velocity norm (MVN) type," *Adv. Robot.*, vol. 30, no. 6, pp. 416–430, Mar. 2016.